Effect of Iron Tailings as Fine Aggregate and Mineral Admixture on Strength and Microstructure of Cement Mortar

Lijuan Kong[1,2]*, Shuheng Xie[1], Caihui Wang[1] and Lihuan Wang[3]

Abstract

To investigate the application of iron tailings in cement-based materials as fine aggregate and mineral admixture, six iron tailings sands were selected from different places of origin, and the methods of acid and alkali activation were adopted to increase the activity of tailings powder. The strength of mortar was evaluated and the composition and microstructure were analyzed to explore the mechanism. The experimental results show that iron tailings sands had little adverse effect on the mortar strength, and there was a maximum increase of 13.2% in 28-day compressive strength compared with that of river sand mortar. The hardness values of all the iron tailings sand and the interfacial transition zone (ITZ) around them were higher than that of natural river sand, but their Ca/Si ratios in the ITZ was lower, indicating a chemical reaction occurred between the iron tailings and cement paste. Generally, the iron tailings sand with higher SiO_2 content and finer particles tend to have higher activity. In addition, the pozzolanic activity of iron tailings powder could be greatly promoted by chemical activation, especially by acid activation. The activity index of cement mortar with unactivated iron tailings powder was only 63% at 28 days, whereas that of acid-activated and compound-activated samples reached up to 93%, and the heights of the maximum heat flow peak of these samples were even higher than that of the control sample without iron tailings powder, and the time to reach the peak was in some advance, moreover their impedance parameters were close to the control sample.

Keywords Iron tailings, Interfacial transition zone, Chemical activation, Mortar strength, Reactivity

1 Introduction

Around the world, a huge amount of tailings is produced every year with continuous mining, which has become the main part of industrial solid waste. However, the tailings contain a large number of silicate minerals, which can be recycled in many fields, especially for the production of building materials (United States Geological Survey—USGS & Mineral Commodity Summaries, 2020; Yang et al., 2014). In China, only just the iron tailings stockpile has exceeded 100 billion tons, and increased by about 80 million tons every year, which not only occupies lots of lands, but also pollutes the environment (Shi et al., 2008). Meanwhile, as one of the most important building materials, concrete has been worldwide applied in infrastructure construction and needs larger amounts of aggregates and cement as raw materials, which not only consumes massive natural resources (e.g., limestone and clay), but also causes serious environmental damage and pollution. The nitrogen oxides from rock blasting and carbon dioxide from cement calcination lead to the pollution of the air and the greenhouse effect (Liu

*Correspondence:
Lijuan Kong
klj@stdu.edu.cn; konglijuan_888@163.com
[1] School of Materials Science and Engineering, Shijiazhuang Tiedao University, Shijiazhuang 050043, China
[2] State Key Laboratory of Mechanical Behavior and System Safety of Traffic Engineering Structures, Shijiazhuang Tiedao University, Shijiazhuang 050043, China
[3] Hebei Institute of Civil Air Defence Works Design and Research, Shijiazhuang 050021, China

Kong *et al. Int J Concr Struct Mater* (2023) 17:24

Page 2 of 16

et al., 2020). Researchers worldwide are exploring various supplementary cementitious materials minimize the use of cement, such as fly ash, slag, silica fume, waste glass, and marble powder, etc. (Ashish, 2019; Ashish & Verma, 2019; Mehta & Ashish, 2020; Thomas et al., 2021). Therefore, the application of tailings in cement-based materials can reduce the problems of resource shortage and environmental pollution, as well as the huge costs for the disposal of tailings in the mining industry.

The particles smaller than 4.75 mm of tailings can be used as the fine aggregate for cement mortar/concrete (Zhang et al., 2020; Zhu et al., 2022). Tian (Tian, 2010) analyzed the composition of iron tailings in Beijing and found that its mineral compositions are mainly quartz, pyroxene, feldspar, etc., with stable chemical properties and qualified physical properties, which could be used as sand in construction to prepare the concrete of C20–C50. Although the higher content of stone powder in tailings leads to the worse fluidity of fresh concrete, it can be adjusted by adding the superplasticizer to meet the requirement of workability (Shettima et al., 2016). In addition, Cai et al. (2009) found that the strength of concrete with a high water/cement ratio had a little increase by using iron tailings to completely replace natural sand, whereas that of concrete with a low water/cement ratio had a slightly decrease. For ultra-high strength concrete, the iron tailings had little effect on concrete strength when its content was less than 20%, beyond this content, the strength decreased almost linearly (Zhao et al., 2014). This should be related to both the property of tailings and the microstructure of the interfacial transition zone (Duan et al., 2013). However, there are great differences in the properties of tailings in different regions, which result in different effects on the performance of concrete.

The fine powder in the tailings can also be used as a mineral admixture to replace partial cement (Adiguzel & S. Tuylu S et al., 2022). However, the activity of iron tailings powder was lower than that of slag and its particle shape being not as round as fly ash. In addition, there are some ways to enhance the activity of tailings, like physical activation, chemical activation, and thermal activation (Saedi et al., 2020). Mechanical grinding can change the crystal lattice of tailings and increase their specific surface area (Saedi et al., 2023); thus, promoting the pozzolanic reaction of tailings powder in cement-based materials. The pozzolanic activity index (28 d) of the activated iron ore tailings was lower than ground granulated blast furnace slag, but qualified for usage as active mixture in cement (Yao et al., 2020). Considering the large energy consumption of high-temperature calcination (Zhou et al., 2022), chemical activation is usually adopted, which has been widely used for increasing the activity of fly ash, slag, and so on (Ishwarya et al., 2019).

Alkaline reagents (e.g., NaOH, KOH, and $Ca(OH)_2$) and sulfates (e.g., Na_2SO_4, $CaSO_4 \cdot 2H_2O$) are he commonly used activators (Zhang et al., 2022), which promote the disintegration of the silicate network structure of the tailings powder, and then the dissolved silicon and aluminum ion clusters can react with hydration products (Chen et al., 2022). When cement is substituted by 10%, 20% 30%, and 40% of mechanochemically activated tailings, respectively, the compressive strength of concrete shows a downward trend with the increase in cement substitution rate but can meet the design requirement (Cheng et al., 2016). Besides, the activity of fly ash can also be enhanced by acids (Losey et al., 2018; Ma et al., 2021). Obviously, most of the research has been done on slag and fly ash, there were few studies about the tailings, especially the acid-activated tailings. The use of unprocessed tailings as a replacement for cement does not obtain desired properties of concrete.

In this study, the iron tailings from different regions in Hebei Province of China were selected to investigate the application of iron tailings in cement-based materials as fine aggregate and mineral admixture. Moreover, the methods of acid and alkali activation were adopted to increase their pozzolanic activity. The strength and activity index of iron tailings mortar were detected, and techniques, such as Scanning Electron Microscopy-Electron Dispersive Spectrometry (SEM–EDS), X-ray Diffraction (XRD), Fourier Transform Infrared Spectroscopy (FTIR), Thermogravimetric Analysis (TGA), Electrochemical Impedance Spectroscopy (EIS) were adopted to characterize the composition and microstructure of samples, and its mechanism was discussed. The object of the study is to promote the application of industrial solid waste in building materials and reduce the environmental damage and pollution caused by tailings stockpiling and massive consumption of aggregates and cement. The results obtained are expected to provide theoretical guidelines for the re-utilization of tailings.

2 Experimental Procedure
2.1 Raw Materials
The cement used was Ordinary Portland Cement (P·O 42.5), which complied with the requirement of Chinese standard GB175-2007. The iron tailings (FN, PS, CD, BD, and LY) were selected from different regions in Hebei Province of China, as shown in Fig. 1, and the natural river sand (TR) was used to make a comparison. Their chemical compositions and physical properties were listed in Tables 1 and 2, respectively, and their particle size distribution were presented in Fig. 2, which could meet the requirement of Chinese standard (GB/T 14684/2022) of "Sand for construction". The iron tailings had stable chemical properties and their bulk
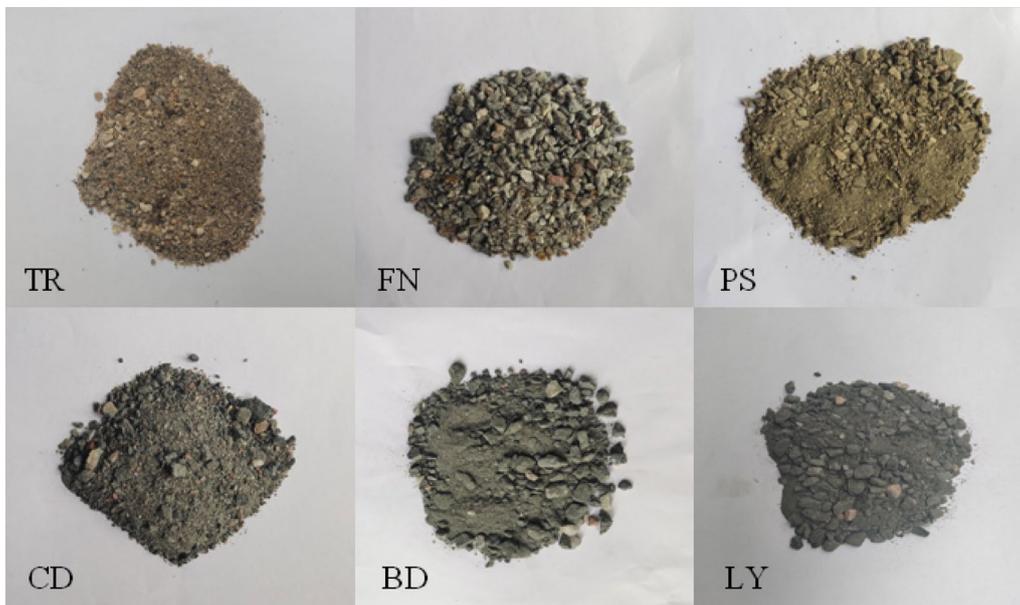
Kong *et al. Int J Concr Struct Mater* (2023) 17:24

Page 3 of 16

Fig. 1 Natural river sand and iron tailings sand samples

Table 1 Chemical compositions of fine aggregates (%)

Serial number	SiO_2	Al_2O_3	Fe_xO_y	CaO	MgO	K_2O	SO_3	Na_2O	P_2O_5
TR	74.3	5.2	3.8	9.1	2.9	0.7	0.1	0.1	0.1
FN	58.2	18.0	6.1	4.8	2.4	4.9	1.2	1.1	0.2
PS	56.9	15.2	11.9	4.7	3.7	4.2	0.2	1.9	0.2
CD	61.1	8.9	13.3	6.0	5.7	1.9	0.3	1.2	0.7
BD	58.7	14.4	11.1	4.3	3.8	3.8	0.1	2.2	0.3
LY	57.2	13.0	12.7	5.3	4.2	3.5	0.2	2.4	0.3

Table 2 Physical properties of fine aggregates

Serial number	Fineness modulus	Bulk density (kg/m^3)	Apparent density (kg/m^3)	MB value	Stone powder content (%)	Crush index (%)	Water absorption (%)
TR	2.6	1427	2820	0.6	2.00	10	1.39
FN	3.9	1455	2750	0.7	1.82	16	2.39
PS	3.0	1569	2775	1.6	4.62	17	2.49
CD	2.7	1650	2760	0.6	4.88	18	0.79
BD	2.4	1530	2885	0.9	8.30	15	1.96
LY	2.8	1590	2870	0.5	7.10	13	3.54

densities were slightly heavier than that of river sand. The polycarboxylate-based superplasticizer was used to adjust the fluidity of fresh mortars. In addition, the iron tailings powder LY was selected as mineral admixture to prepare mortar and its specific surface area was 384 m^2/kg.

2.2 Specimen Preparation and Tailings Activation

The iron tailings sand was used as fine aggregate to prepare cement mortar, and the river sand was used for comparison, and a prefix letter G and D, corresponding to the water/binder ratios of 0.48 and 0.34, was added to name the mortars prepared with them. The fluidity of
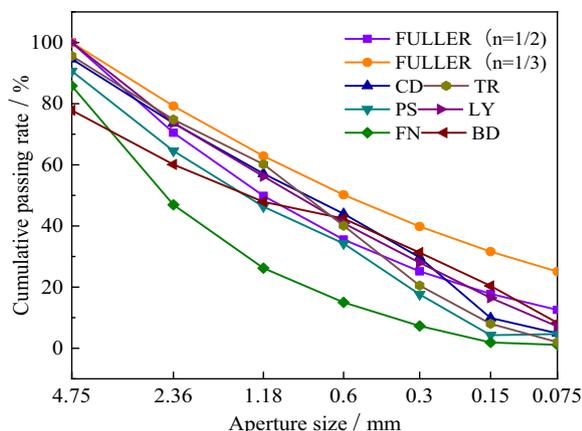
Kong *et al. Int J Concr Struct Mater* (2023) 17:24

Page 4 of 16

Fig. 2 Particle size distribution of fine aggregates

fresh mortar was controlled within 190–210 mm, and then cast in the molds of 4.0 cm × 4.0 cm × 16.0 cm. After curing (at 20 °C and 95% relative humidity) for 7 and 28 days, the specimens were tested for strength. In addition, the iron tailings powder was used as a mineral admixture to replace 30% cement in the preparation of cement mortar with water/binder ratio of 0.5. In this case, the ISO standard sand was used to compare the activity of tailings powder. Tailings powder FN with a relatively lower activity and higher stone powder content was selected to take activation by NaOH and HCl in different ways. The details are as follows: (i) Activation method A: The solid activator dosages were 1%, 3%, 5% by the weight of tailings powder respectively, and they were added directly in the process of mortar preparation; (ii) Activation method B: First, the alkali activator was prepared by mixing 0.3 g, 0.9 g, 1.5 g solid NaOH and 0.8 g, 2.4 g, 4.1 g HCl solution (36–38% content) with 15 mL deionized water, respectively. Then, the tailings powder weighing 30 g was immersed in

each activator solution and then dried at 105 °C after water bath heating for 10 h to prepare the mortar. (iii) Activation method C: This activation method was the same as above (method B), except the activated tailings need to be washed to neutral with deionized water, and then dried for mortar preparation.

For iron tailings powder samples, their names are composed of the following parts: the letter "W" represents the iron tailings powder, "N/H" represents the powder by alkaline or acid activation; "A/B/C" represent different activation methods; number "0/1/3/5" represents the dosage of activator.

2.3 Test Methods

2.3.1 Compressive Strength and Activity Index

The compressive strength of the mortar specimens was measured according to Chinese standard (GB/T 17671-2021) of "Test method of cement mortar strength (ISO method)". Furthermore, the activity index of tailings can be calculated by comparing the strength ratio of test mortar to control mortar according to GB/T 1596-2017.

2.3.2 Nano-indentation

The hardness of the fine aggregate, hardened cement paste and the interfacial transition zone (ITZ) between them was tested by nano-indenter (KLA iMicro), as shown in Fig. 3a Before testing, the sample should be first polished with 400, 800, and 1200 mesh SiC sand papers orderly to obtain flat surface, and then with 9 μm, 3 μm, and 1 μm oil-based diamond suspension for fine polishing. When considering the heterogeneity of the material, five parallel test lines were made for each sample and each testing interval was 10 μm, see Fig. 3b The Poisson's ratio was 0.17 and the load was 700 mN in testing.
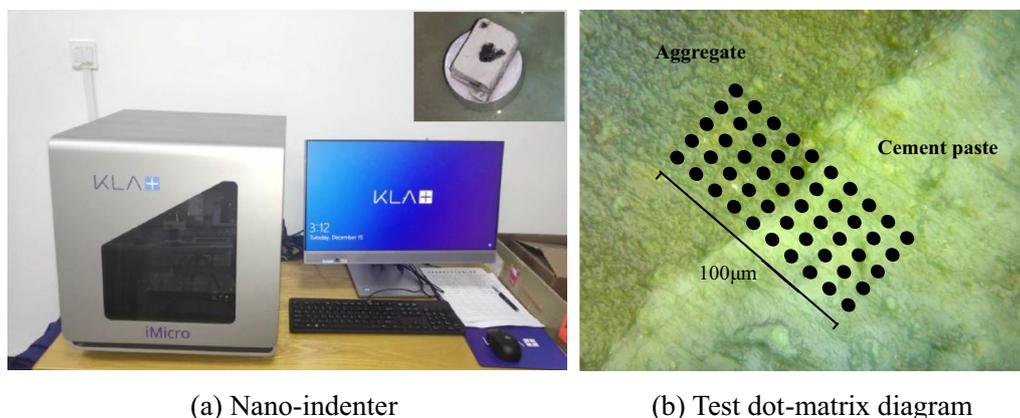

(a) Nano-indenter

(b) Test dot-matrix diagram

Fig. 3 Nano-indentation test

Kong *et al. Int J Concr Struct Mater* (2023) 17:24

Page 5 of 16

2.3.3 SEM–EDS, XRD, FTIR, and TGA Analyses

The morphology and element distribution of the tailings and mortar specimens were analyzed by SEM–EDS (HITACHI, Japan). Before testing, the samples should be dried and gold-coated. The tailings were also grounded into powder and prepared for the XRD (Bruker, Germany) and FTIR (Nicolet, USA) analyses of the change of the compositions in the specimens before and after activation. The spectra measured ranged between $10° < 2\theta < 60°$. The samples with different tailings powder as cement replacement was monitored by TGA (Mettler-Toledo, Switzerland), and the content of calcium hydroxide (CH) and bound water can be calculated. The sample was heated in an N_2 atmosphere at a rate of 10 ℃/min.

2.3.4 Ion Release Concentration Test

To study the effect of chemical activation on iron tailings, an inductively coupled plasma mass spectrometer (ThermoFisher, USA) was used to test and analyze the ion release concentration of the tailings powder in different solutions. The 3 g tailings powder was mixed with 30 ml solution by a magnetic mixer for 2 h and then filtered with a 0.45-μm filter membrane for testing. The acid/alkali solution prepared with the solid activator dosages of 1%, 3%, and 5% was designated as H1, H3, H5, and N1, N3, N5, respectively. The cement solution containing Ca^{2+}, Na^+, Al^{3+}, Si^{4+}, OH^-, and other minor ions was prepared according to the method stated in Ref. (Kong et al., 2014).

2.3.5 Isothermal Calorimetry Test

To investigate the effect of tailings powder on the cement hydration reaction, a TAM Air isothermal calorimeter (TA Instruments, USA) was used to monitor the change of the heat evolved during the hydration process at 20 ℃ for 72 h. The cement paste was prepared at a water/binder ratio of 0.5, and the tailings powder was added 30% wt% concerning cement.

2.3.6 EIS Test

An IM3570 impedance analyzer (HIOKI, Japan) was adopted to study the EIS of the cement mortar, which can reflect the microstructure of the cement mortar (Ping et al., 1994). The impedance was measured from 5 MHz down to 1000 Hz, and the amplitude of the sinusoidal voltage was chosen to be 10 mV. The size of the test samples is 2 cm × 2 cm × 2 cm, and they should be vacuum water saturated before testing.

3 Results and Discussion

3.1 Influence of Iron Tailings on Mortar Strength

3.1.1 Compressive Strength of Mortars

Fig. 4 presents the 7-day and 28-day compressive strength of the mortars prepared with different fine aggregates. For the mortar with a water/binder ratio of 0.48, GBD had the highest strength, and its 28-day compressive strength was 13.2% higher than that of GTR, followed by GCD, which increased by 10.5%. For the mortar with a water/binder ratio of 0.34, DCD had the highest strength, and its 28-day compressive strength was 10.0% higher than that of DTR. However, both the 7-day and 28-day strengths of DFN were lower than that of DTR, and the reductions were 8.1% and 2.1%, respectively. Using iron tailings as fine aggregate in cement mortar had little adverse effect on the mortar strength, and even promoted the growth of the strength, especially for the mortar with a high water/cement ratio. This is consistent with the results obtained by Zhang (2020) that replacing river sand with iron tailings did not make any significant impact on the general properties of concrete, the slump
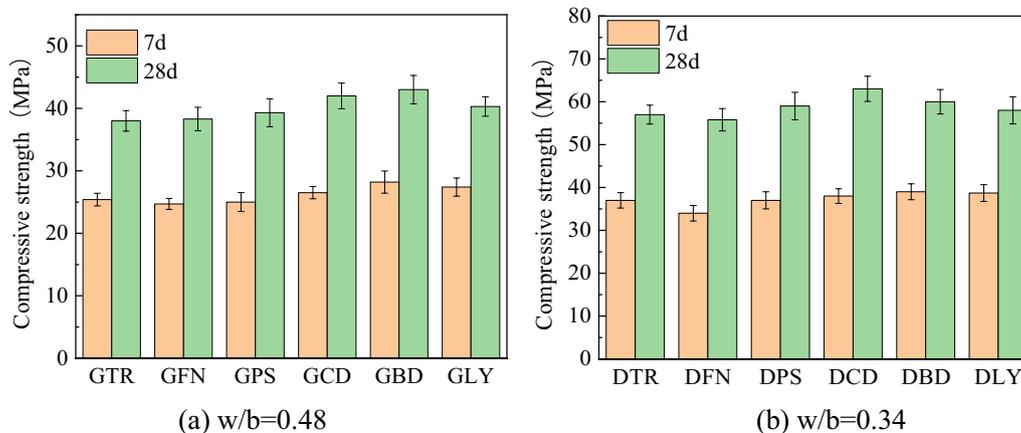

(a) w/b=0.48   (b) w/b=0.34

Fig. 4 Compressive strength of iron tailings mortar

Kong *et al. Int J Concr Struct Mater* (2023) 17:24

Page 6 of 16

of iron tailings sand concrete was a litter lower than river sand concrete, while the strength was slightly improved.

3.1.2 Nano-Hardness of the ITZ

In view of the mortar with a high water/binder ratio usually has a weaker ITZ, the mixture series "G" was selected to investigate the mechanism of the effect of iron tailings on mortar strength. The nano-hardness of the tailings, hardened cement paste, and the ITZ between them were tested, as shown in Fig. 5a, and each data in the figure was the average of five test values.

It can be seen that the hardness of the aggregates was in the range of 5–10 GPa, significantly higher than that of the cement paste matrix of about 1.5 GPa, moreover, the hardness of all the iron tailings was higher than that of natural river sand, and the hardness of GPS was almost two times of GTR. In addition, all the samples had the lowest hardness in the ITZ, which was only about 0.5 GPa. To further compared their difference, Fig. 5b shows the hardness of the interface between aggregate and cement paste, and that of the ITZ ranged from the interface to the distance of 40 μm. The interface hardness of the tailings sand was higher than that of the river sand, except for GLY, and the ITZ hardness of GCD and GBD was also slightly higher than that of GTR. This may be one of the reasons for their good compressive strength (Fig. 4).

3.1.3 Element Distribution of the ITZ

EDS was carried out to investigate the elemental distribution in the ITZ around different fine aggregates, and the positions at the distance of 0 μm, 25 μm, and 50 μm from
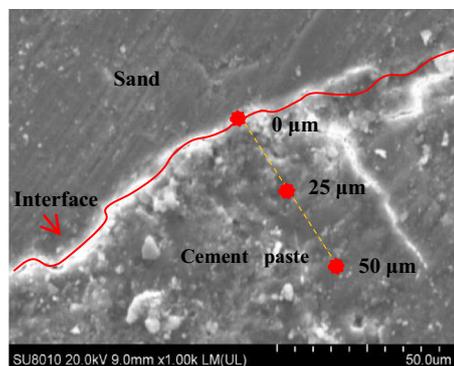

Fig. 6 Schematic diagram of the EDS test

the interface were detected, as shown in Fig. 6. Six points were tested at each distance, and their average was used.

Fig. 7 shows the EDS test results of the ITZ around river sand (TR) and tailings sand (CD). Obviously, the content of Si and Al at the interface between tailings sand and hardened cement paste was higher than that of natural sand, and they had some decrease at the position 25 μm away from the CD surface, which was contrary to that of the ITZ around TR. To the distance of 50 μm from the aggregate surface, the difference in their element compositions was no longer significant, indicating the dissolution of elements silicon and aluminum from the tailings surface.

Table 3 lists the Ca/Si ratio of the ITZ around different fine aggregates. It can be seen that the Ca/Si ratio of sample GCD at the interface was only 0.65, significantly lower than that of the other samples, followed by GBD of 0.98, while that of GFN and GLY was comparable to GTR of about 1.5. The Ca/Si ratio of all the samples increased
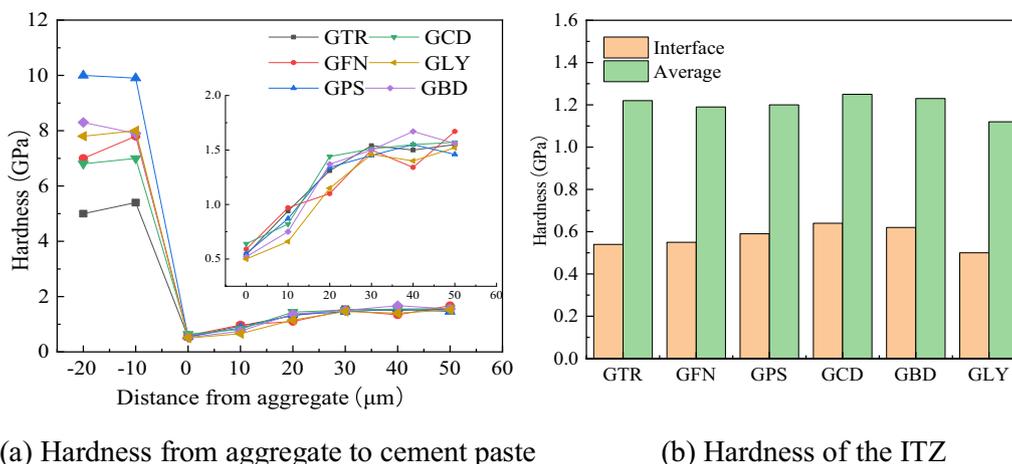

(a) Hardness from aggregate to cement paste

(b) Hardness of the ITZ

Fig. 5 Nano-indentation test

Kong *et al. Int J Concr Struct Mater*   (2023) 17:24

Page 7 of 16

(a) TR-0 μm

(b) CD-0 μm

(c) TR-25 μm

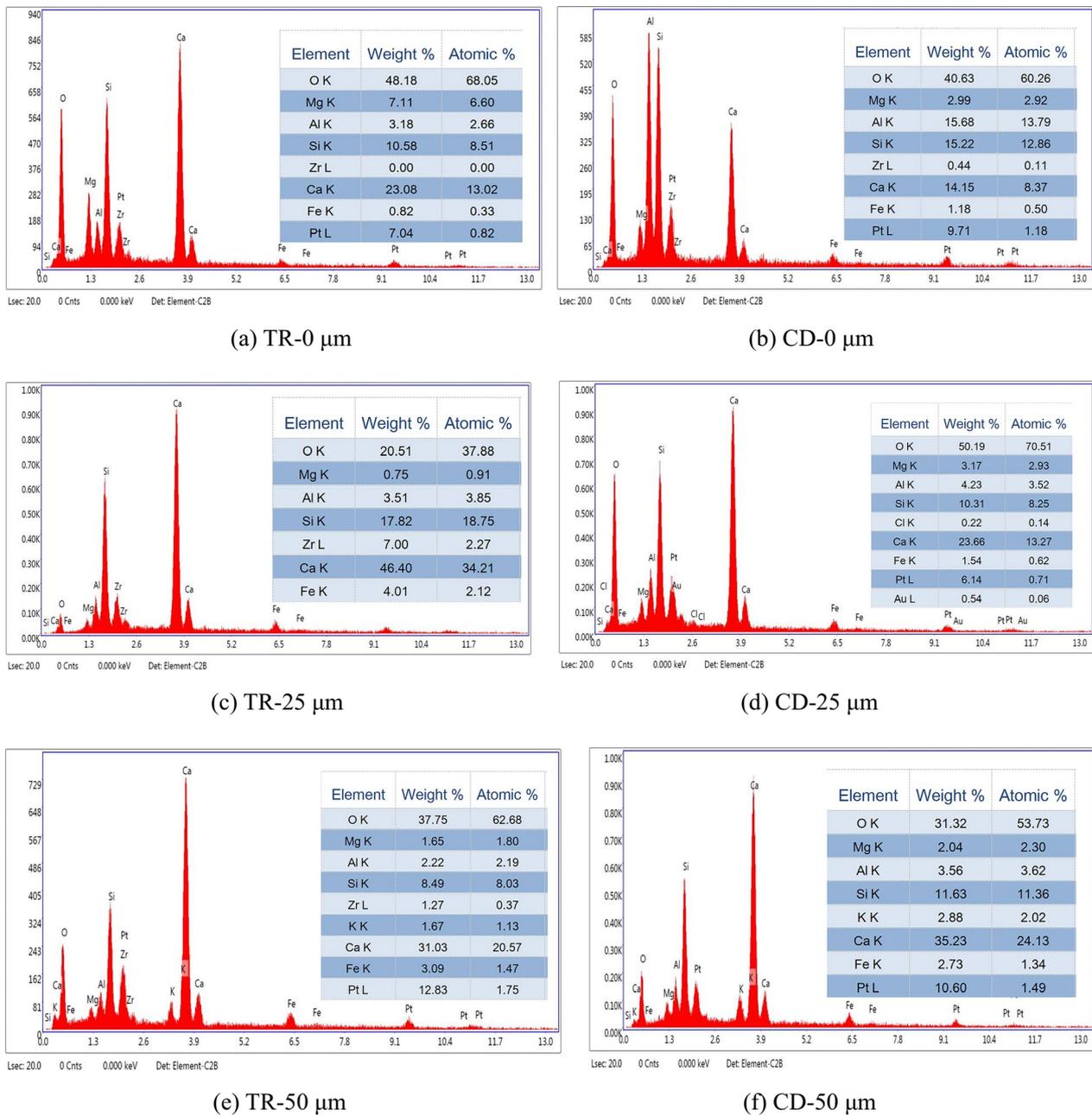
(d) CD-25 μm

(e) TR-50 μm

(f) CD-50 μm

Fig. 7 EDS analysis of the ITZ around natural and tailings sand

gradually with the increase of the distance from the aggregate surface, and by the distance of 50 μm that of the tailings sand samples was still lower than that of the natural sand sample, but their gap had been narrowed greatly. This should be related to the broken of Si–O–Si bonds in iron tailings (Wu, 2020), resulting in a higher activity than natural sand. The iron tailings could have a chemical reaction with the cement paste, and the products formed around the aggregate led to a higher ITZ

hardness and mortar strength than the sample with river sand.

3.2 Influence of Chemical Activation on Tailings Powder
3.2.1 Ion Dissolution
Fig. 8 presents the results of the ion dissolution of iron tailings in acid and alkali solutions with different concentrations. Obviously, the ion release concentrations of iron tailings in acid solutions were significantly higher than

Kong *et al. Int J Concr Struct Mater*   (2023) 17:24

Page 8 of 16

that in alkali solutions, moreover, they increased with the increase of acid concentration, and an increase of 30.7%, 114.5%, and 23.1% in H5 compared to H1 for Al^{3+}, Si^{4+}, and Ca^{2+}, respectively. However, a higher alkali concentration would inhibit the ion dissolution of tailings. The concentrations of the Al^{3+}, Si^{4+}, and Ca^{2+} for N5 were similar to that for N1, even slightly lower, whereas the concentrations of Si^{4+} and Ca^{2+} for N3 were significantly higher compared to the others. This suggests that the acid is more destructive to the structure of iron tailings

than alkali, and the leaching ions would probably react chemically and form a passive film adhered to its surface in an environment of a high alkali concentration.

Figs. 9 and 10 present the results of the ion dissolution of different iron tailings powder (see Sect. 2.2) in deionized water and cement solution. From Fig. 9 it can be seen that the concentration of released ions from activated iron tailings powder in deionized water was significantly higher than that of unactivated ion tailings (W0). This indicates that the mineral structure was destroyed

Table 3 Ca/Si ratio of the ITZ

Distance from interface	Ca/Si					
	GTR	GFN	GPS	GCD	GBD	GLY
0 μm	1.53	1.50	1.24	0.65	0.98	1.60
25 μm	1.82	1.92	1.76	1.61	1.55	1.84
50 μm	2.56	2.36	2.23	2.12	1.98	2.46
Average	1.97	1.93	1.74	1.44	1.50	1.96

(a) Al^{3+} (b) Si^{4+} (c) Ca^{2+}
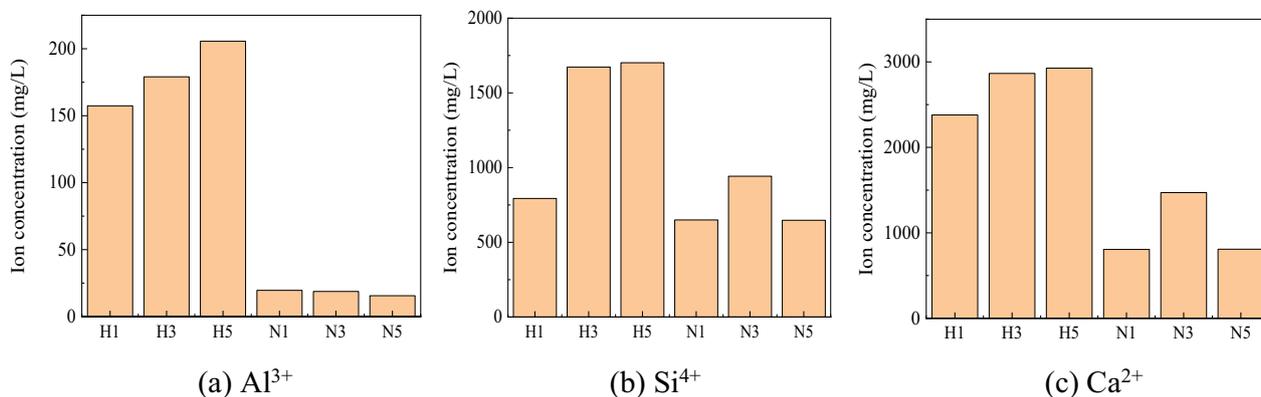
Fig. 8 Ion release concentration of iron tailings in different activated solutions

(a) Al^{3+} (b) Si^{4+} (c) Ca^{2+}
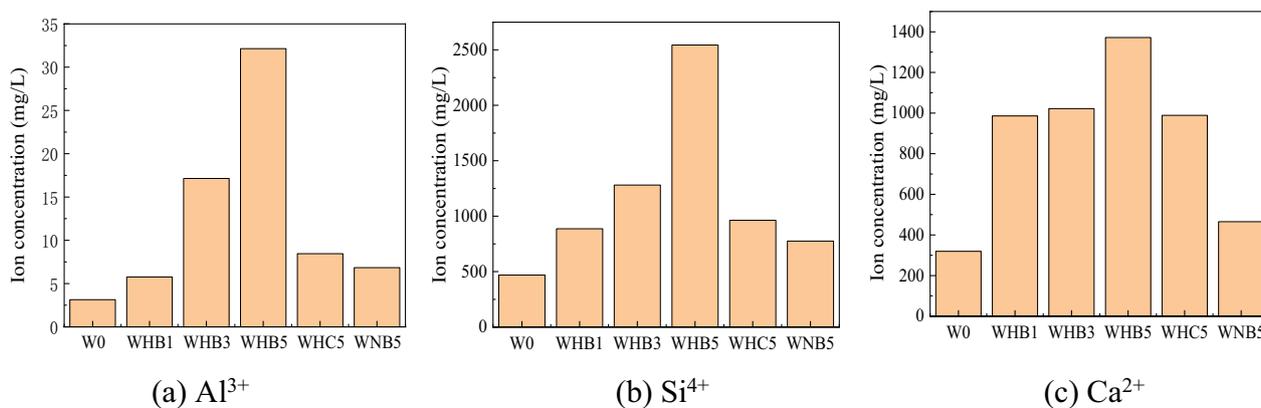
Fig. 9 Ion release concentration of iron tailings in deionized water

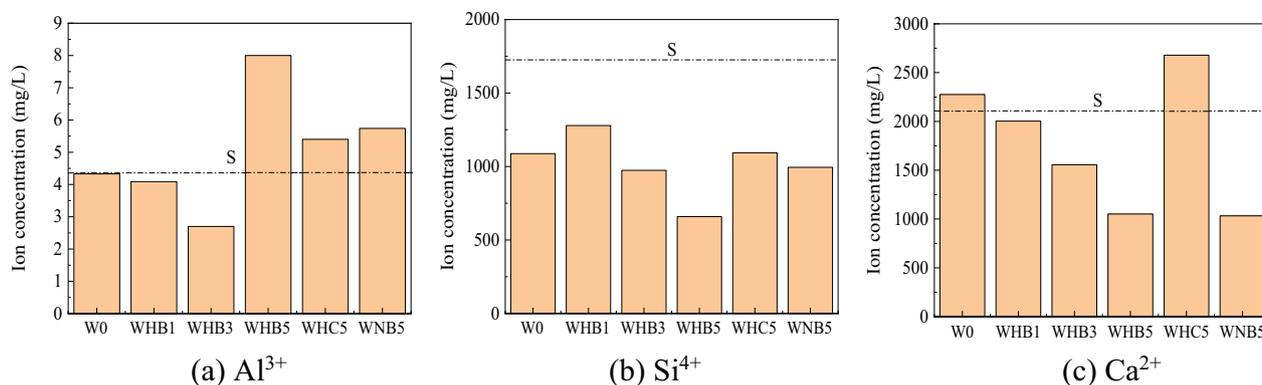(a) Al^{3+} (b) Si^{4+} (c) Ca^{2+}

Fig. 10 Ion release concentration of iron tailings in cement solution

by chemical activation and some Si–O/Al–O bonds were broke, thus the dissociation degree of tailings was greatly increased. With the increase of the concentration of activator solution used for immersing iron tailings powder, the content of released Al^{3+} and Si^{4+} increased significantly, and that of WHB5 was about 5–8 times of W0. The ion release concentration of activated iron tailings after rinsing had a great decrease, and that of WHC5 was only comparable to WHB1. Moreover, the ion release concentration of iron tailings activated by 5% NaOH and after rinsing treatment (WNB5) was greatly reduced, indicating that the activity of the iron tailings powder activated by alkali was lower than that by acid.

Fig. 10 shows the results of the ion release concentration of the samples in cement solution (S), which were a different form that in deionized water, and should be the sum of the ion concentrations of sample S and that in Fig. 9 if no reaction occurred. However, if the results were higher or lower than their sum, indicating that the cement solution promoted or inhibited the ion dissolution, or had a chemical reaction consuming the ions. Obviously, the Al^{3+}, Si^{4+}, and Ca^{2+} concentrations of the tailings samples in the cement solution were lower than the sum of that in deionized water and pure cement solution, which should be due to the reaction occurred

between the iron tailings powder and cement solution, and the generated products were filtered out. Furthermore, the reactivity of iron tailings powder after activation was higher than that of unactivated sample W0, especially for acid-activated samples, and that increased with the increase of acid concentration and decreased by the rinsing after activation.

3.2.2 Morphology and Composition
Fig. 11 shows the morphology of the tailings powder samples. The tailings power unactivated was designated as W0, and that activated by NaOH and HCl with a dosage of 5% (method B) were designated as WNB5 and WHB5, respectively. Obviously, the morphology of tailings powder had become rougher after 1-h immersion in an alkali/acid solution, the particle was partially disintegrated and some micropores were formed on the surface.

Fig. 12 presents the results of the FTIP spectra of the tailings powder samples. The bands at 3440 cm^{-1} and 1630 cm^{-1} are related to the Si–O–H and O–H stretching and bending vibrations of molecular water, respectively (Jiang, 2008). These absorption bands for the W0 sample were very weak, while that for the WHB5 sample was stronger. An absorption band at 1444 cm^{-1} appeared for the W0 sample, which is related to the asymmetric
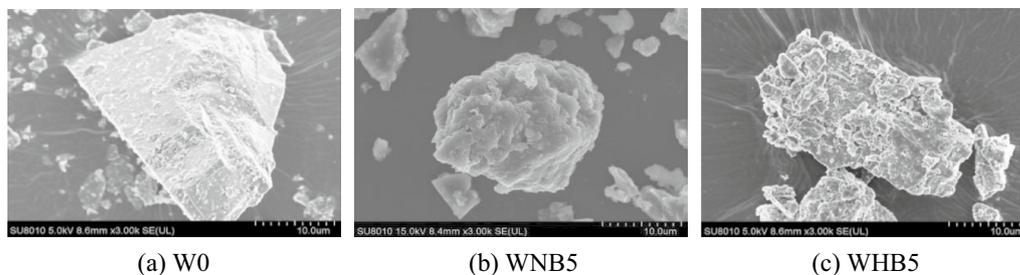

(a) W0   (b) WNB5   (c) WHB5

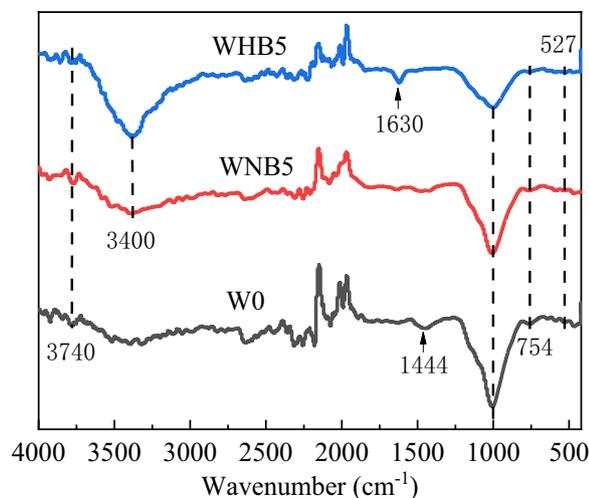**Fig. 11** Morphology and element composition of tailings powder

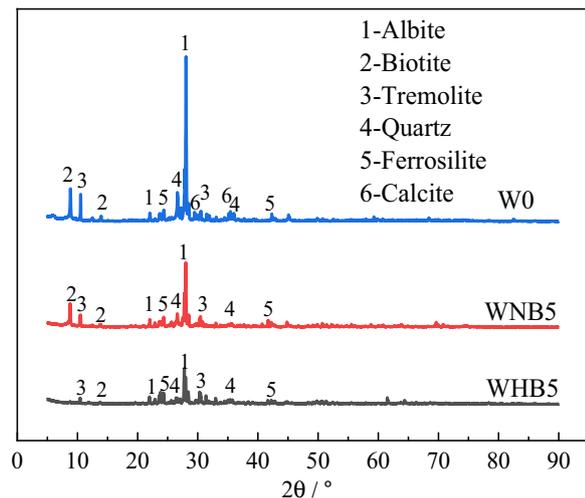**Fig. 12** FTIR spectra of unactivated and activated tailings powder

Fig. 13 XRD pattern of the unactivated and activated tailings powder

stretching vibration of CO_3^{2-}. It is speculated that the iron tailings contain a small amount of calcite. However, this band disappeared after acid activation. In addition,

there was a sharp and very intense absorption band at 1010 cm^{-1}, which corresponds to the asymmetric stretching vibration of Si–O–Si(Al), and this band was weakened slightly after activation, especially for WHB5. Obviously, the integrity and symmetry of mineral crystals were affected, and the Si–O, and Al–O bonds were destroyed by chemical activation.

Fig. 13 shows the XRD pattern of tailings power samples. Their main mineral compositions are albite, quartz, tremolite, and so on. However, the diffraction peaks of WHB5 and WNB5 were all weakened compared with control W0, especially that of albite, indicating that the crystal structure was destroyed and the degree of amorphous increased.

To study the effect of chemical activation on the crystal structure of tailings, the crystallinity (K) of the main mineral was calculated based on the ratio of the diffraction peak intensity of activated and unactivated tailings (Pu, 2017). Zhang et al. (2022) found that NaOH has superior performance in reducing the crystallinity and surface binding energy of iron ore tailings. From the results listed in Table 4, it can be found that the crystallinity of all the minerals decreased after chemical activation, and the acid activation (WHB5) had more serious damage to the crystal structure than alkaline activation (WNB5). In other words, the chemical activation increased the amorphous degree of these minerals, and the potential activity of iron tailings was greatly activated by acid. For sample WHB5, the crystallinity of biotite in iron tailings was only 9.82% after acid activation, and that of tremolite and quartz was about 24%.

3.3 Influence of Tailings Powder on Cement Mortar
3.3.1 Activity Index
Fig. 14 presents the 28d activity index results of the cement mortar prepared with iron tailings powder that is activated by HCl and NaOH of different dosages and methods. Obviously, the chemical activation on iron tailings powder increased the activity index of mortar in various degrees except for NA5. The activity index of cement mortar with unactivated iron tailings powder (W) was

Table 4 Crystallinity of the main phase of tailings

Mineral composition	2θ/°	W0		WHB5		WNB5	
		Intensity/CPS	K/%	Intensity /CPS	K/%	Intensity/CPS	K/%
Biotite	8.85	9056	100.00	889	9.82	6628	73.19
Tremolite	10.55	7284	100.00	1802	24.73	3412	46.84
Quartz	26.59	7796	100.00	1902	24.40	3918	50.26
Albite	22.03	2535	100.00	2221	87.61	2376	93.72
	27.84	14,480	100.00	6133	42.3	9829	67.87
	28.07	46,370	100.00	10,201	22.00	17,498	37.73

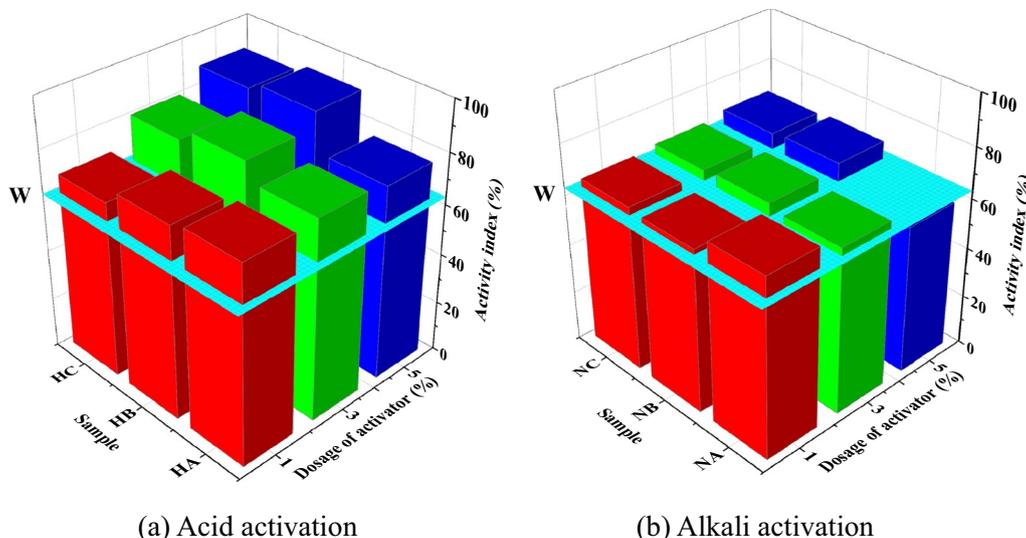(a) Acid activation

(b) Alkali activation

Fig. 14 Activity index of cement mortar with single-activated iron tailings powder

only 63% ($\leq$ 65%), unqualified for usage as active mixture in cement, whereas that of mortars with activated tailings powder was almost all higher than 70% and even as high as 92.5% for HB5. Yao et al. (2020) conducted the mechanical activation on iron ore tailings and found that the pozzolanic activity index was 73.4%. The effect of acid activation on the increase of the activity of iron tailings is more significant than that of alkali activation. In addition, the iron tailings powder directly mixing into the cement mortar after immersion in acid solution (HB) had a notable effect on the increase of activity index, and the higher the acid concentration was, the better the excitation effect would be. However, the high dosage of alkali activator was adverse to the mortar strength, and the activity index of NA1 sample was significantly higher than the others.

Based on the single activation results, better activation methods (HB5, NB5, and NA series) were selected and combined to investigate the compound activation on the activity index of mortar with iron tailings powder. For NB5HB5, the tailings powder were immersed first by alkaline solution then by acid solution, whereas for HB5NB5, the immersion order was exchanged. For HB5NA1, HB5NA3, and HB5NA5, the tailings powder was immersed by acid solution and the solid NaOH with different dosages of 1%, 3%, and 5% was also added directly into the mortar. From the results shown in Table 5, it can be seen that the activity indexes of the cement mortar prepared with iron tailings powder by compound activation were higher than that by single activation. Among them, the activity index of HB5NA3 was the highest and could reach up to 92% at the age of 3 days, but little growth after

Table 5 Activity index of cement mortar with compound-activated iron tailings powder

Serial number	Activation type	Activity index /%	
		3d	**28d**
NB5HB5	NaOH (5%) + HCl (5%)	87	88
HB5NB5	HCl (5%) + NaOH (5%)	91	90
HB5NA1	HCl (5%) + NaOH (1%)	89	91
HB5NA3	HCl (5%) + NaOH (3%)	92	93
HB5NA5	HCl (5%) + NaOH (5%)	82	79

that, indicating that compound activation can greatly improve the early activity of iron tailings powder.

3.3.2 Hydration Reaction

Fig. 15 represents the isothermal calorimetric curves for the control cement containing no mineral admixture and for cement containing different iron tailings powder. From Fig. 15a, it can be seen that the control sample J first reached the minimum heat flow peak at about 1.4 h and shifted into the acceleration period, whereas the addition of iron tailings powder in samples extended this time. The heat flow of the W sample with unactivated iron tailings was the lowest whether in the induction period or acceleration period, whereas that of the NA3 sample with alkali-activated iron tailings powder was higher in the induction period and the first reached the maximum heat flow peak, indicating that the NaOH brought in by tailings powder promoted the cement hydration, but the heat flow in both acceleration and
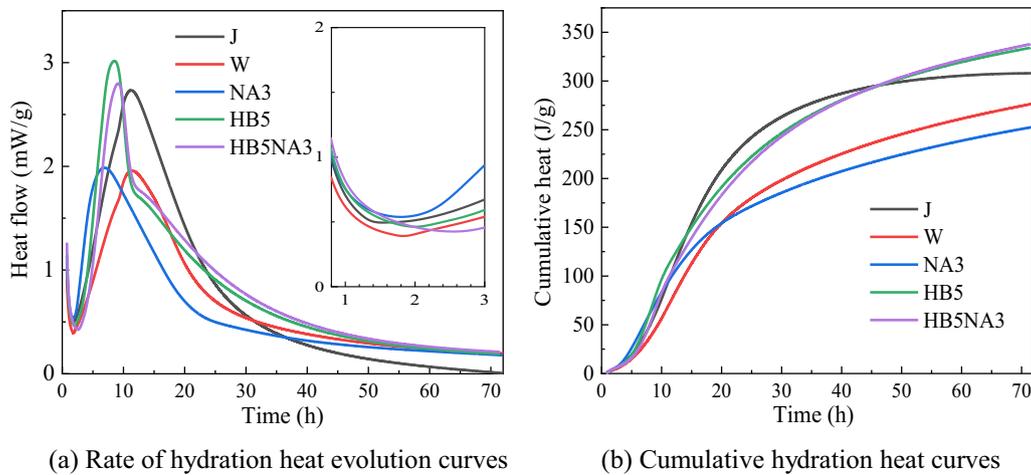
Kong *et al. Int J Concr Struct Mater*   (2023) 17:24

Page 12 of 16

(a) Rate of hydration heat evolution curves

(b) Cumulative hydration heat curves

Fig. 15 Isothermal calorimetric analysis of the cement paste samples

deceleration periods was lower than the other samples. The heights of the maximum heat flow peak of HB5 and HB5NA3 samples were even higher than the control J sample, and the time to reach the peak was also in some advance. Besides, the HB5NA3 showed an almost identical cumulative heat curve as HB5, and both of them had sustained growth in hydration heat, and even exceeded the J sample after about 48 h, as shown in Fig. 15b In general, the cumulative hydration heat of W and NA3 was lower than the other samples, and that of NA3 was the lowest after 20 h, indicating little effect of NaOH on the activity of iron tailings powder.

In addition, the hardened cement paste with different iron tailings powder was tested by TGA at 28 days, and the results are shown in Fig. 16a The weight loss of the samples between 50 and 400 ℃ (TG_1), is mainly due to the dehydration of hydrated calcium silicates (CSH) and

ettringite, and that between 400 and 550 ℃ (TG_2) and 550–770 ℃ (TG_3), are caused by the dehydration of CH, CSH, and ettringite, and the decomposition of the carbonization product. Therefore, the CH and bound water content of the hydrates can be calculated as follows (Li, 2003):

$$M_1 = \left(\frac{TG_2}{18} + \frac{2}{3} \times \frac{TG_3}{44} \right) \times 74 \tag{1}$$

$$M_2 = TG_1 + TG_2 + \frac{TG_3}{3} + \frac{2}{3} \times \frac{TG_3}{44} \times 18 \tag{2}$$

where, M_1 is the content of CH in cement pastes, %; M_2 is the content of bound water in cement pastes, %.

From Fig. 16b, it can be seen that both the contents of CH and bound water of the control sample J were the
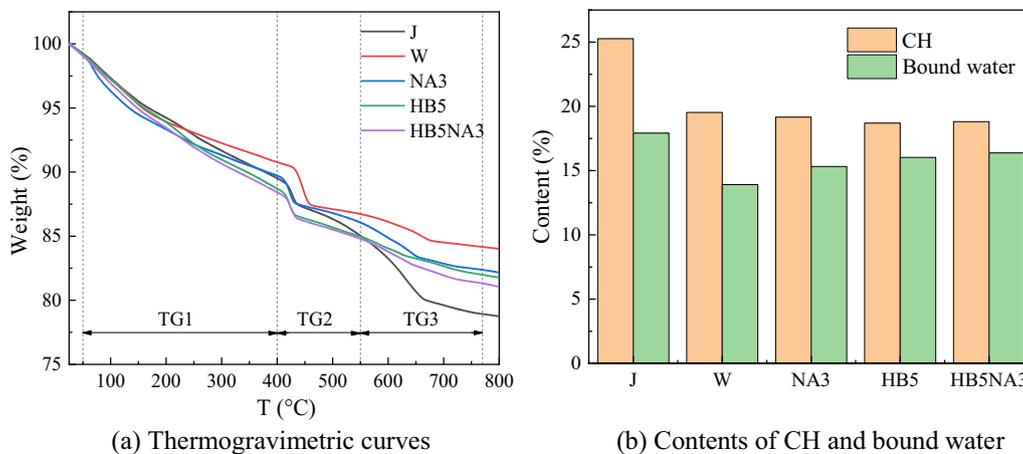

(a) Thermogravimetric curves

(b) Contents of CH and bound water

Fig. 16 Thermogravimetric analysis of the cement paste samples

Kong *et al. Int J Concr Struct Mater* (2023) 17:24

Page 13 of 16

highest, compared with the samples mixed with iron tailings powder. This is because the cement was partly replaced by iron tailings powder, resulting in less generation of CH, and the secondary hydration of iron tailings powder would consume some CH further. Moreover, all the samples with activated iron tailings powder had a lower CH content and a higher bound water content than that with unactivated iron tailings powder. This indicates that the pozzolanic activity of iron tailings powder was greatly promoted by chemical activation; thus, more CH was consumed and more products were generated in the cement hydration. In particular, the HB5 and HB5NA3 samples had a higher reactivity, and their bound water content increased about 17% compared with unactivated sample W, already close to control sample J.

3.3.3 Microstructure

Fig. 17 presents the morphology of the samples with different iron tailings powders. For the W sample with unactivated tailings, the boundary between iron

tailings powder and cement paste was apparent, there was little trace of reaction, and many micropores could be observed in the hardened cement paste (Fig. 17a).

For the NA3 sample with alkali-activated iron tailings, although the clear boundary could also be observed, the surface of iron tailings powder particles was rougher, and some hydrates attached to it, moreover, some CH crystals were formed around the tailings due to the reaction between dissolved Ca^{2+} from iron tailings and OH^- introduced by an activator (Fig. 17b). Furthermore, both the acid activation and acid–alkali combined activation could increase the activity of iron tailings significantly, few unreacted tailings powder particles were left in HB5 and HB5NA3, and it has been difficult to distinguish the boundary between iron tailings powder and dense cement paste (Fig. 17c and d), indicating that most of the iron tailings participated in the cement hydration.

In addition, the microstructure of cement-based materials was characterized by EIS. Fig. 18 presents the Nyquist diagrams of different samples at different age. By
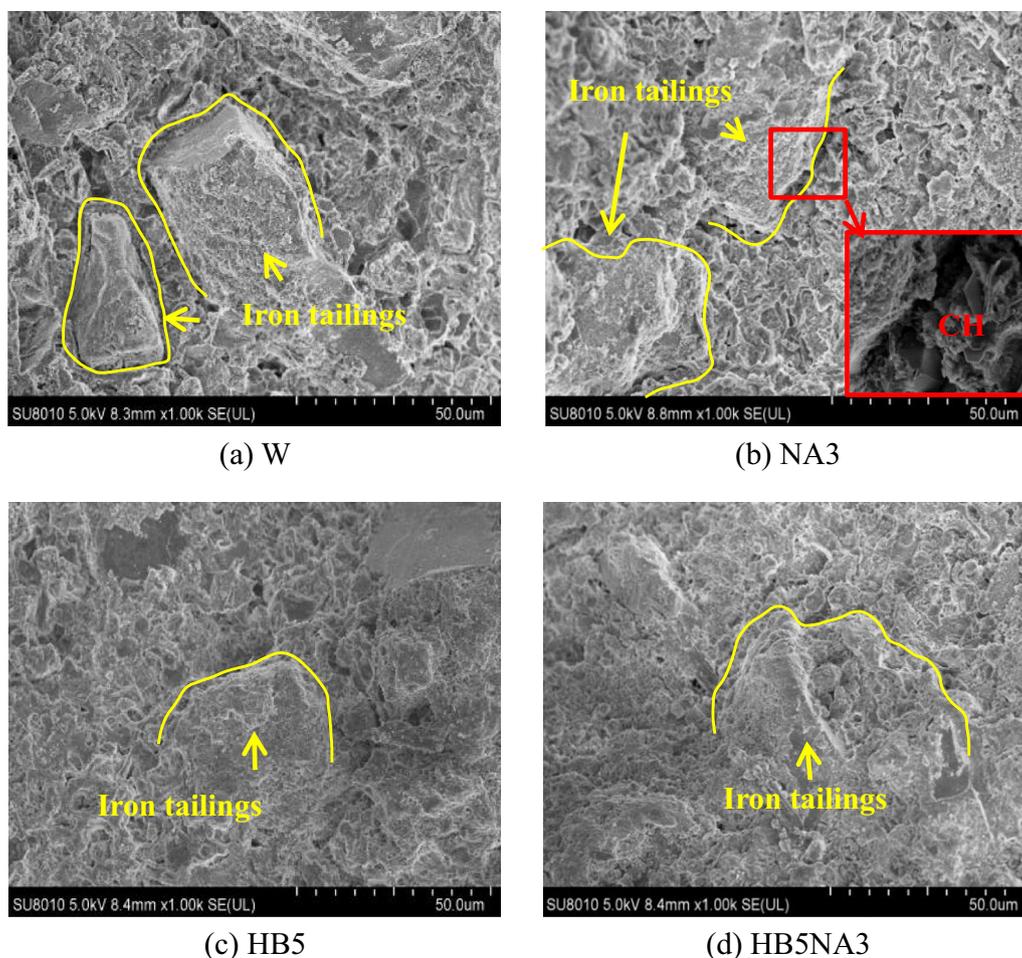

(a) W   (b) NA3

(c) HB5   (d) HB5NA3

Fig. 17 Morphology of the cement paste with different iron tailings powder

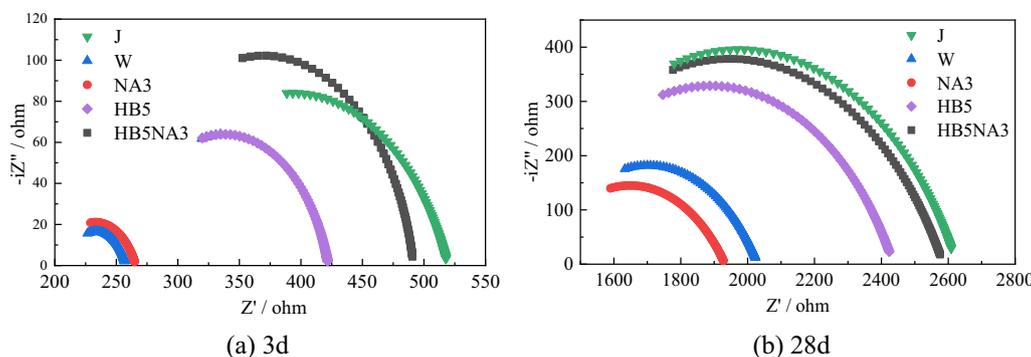Kong *et al. Int J Concr Struct Mater*   (2023) 17:24

Page 14 of 16

Fig. 18 Nyquist diagrams of the EIS test

contrasting the 3 days and 28 days results, both the left coordinate values and high-frequency semicircle diameters had an evident increase with the increase of curing age, reflecting the gradually denser microstructure of materials (Song, 2000). Furthermore, it is obvious that the high-frequency semicircle of the NA3 sample was close to that of the W sample, and both of their diameters were very small, indicating that the activity of alkali-activated tailings powder was very low, similar to unactivated tailings. For HB5 and HB5NA3 samples, their high-frequency semicircle diameters had increased and their positions also shifted to the right. This indicates that the activity of iron tailings powder was greatly improved by acid activation and acid–alkali combined activation, and more hydrated were formed to fill the pores. Particularly in the HB5NA3 sample, its diameter and position had approached or even exceeded that of control sample J without tailings powder.

In addition, the equivalent circuit model parameters (R_0, R_1) were extracted from the impedance spectra using Zview software, and the parameter R_{CCP}, which can reflect the total impedance of all the continuous conduction paths, were calculated by the sum of them and together listed in Table 6. It can be seen that the parameter R_{CCP} of the W sample mixed with 30% unactivated tailings powder was only half of the control cement paste sample J at 3 days, and that of the NA3 sample only had a

slight increase. However, the parameter R_{CCP} of HB5 and HB5NA3 samples had reached 81.3% and 94.6% of the J sample, respectively, indicating a great increase in tailings activity. By the age of 28 days, the R_{CCP} of W, HB5, and HB5NA3 samples had reached 73.4%, 92.5%, and 98.1% of the J sample, respectively. Obviously, the activity of iron tailings had gradually displayed with the increase of curing age, especially for the tailings powder by acid–alkali compound activation, their 28 days microstructure was almost as dense as the cement mortar sample without tailings powder.

4 Conclusions

1. The strength of cement mortar prepared with most of the iron tailings sand was no less than that of the mortar with natural river sand, and even had a maximum increase of 13.2% in 28-day strength. The hardness values of all the iron tailings sand and the ITZ around them were higher than that of natural river sand, but their Ca/Si ratios in the ITZ was lower, indicating a chemical reaction occurred between the breaking bond of Si–O on iron tailings surface and cement paste. The iron tailings sand with a higher SiO_2 content and finer particles tends to have higher activity.

Table 6 Impedance parameters of different samples

Age/d	3d			28d		
Impedance/Ω	R_0	R_1	R_{CCP}	R_0	R_1	R_{CCP}
J	268	251	519	1325	1308	2633
W	209	48	257	1366	566	1932
NA3	207	65	272	1375	656	2031
HB5	253	169	422	1342	1094	2436
HB5NA3	248	243	491	1314	1269	2583

Kong *et al. Int J Concr Struct Mater*   (2023) 17:24

Page 15 of 16

2. The pozzolanic activity of iron tailings powder could be greatly promoted by chemical activation, especially by acid activation. The activity index of cement mortar with unactivated iron tailings powder was only 63% at 28 days, whereas that of acid-activated and compound-activated samples reached up to 93%, and the heights of the maximum heat flow peak of these samples were even higher than that of the control sample without iron tailings powder, and the time to reach the peak was in some advance, moreover their bound water content and impedance parameters were close to the control sample.

3. The dissolution of Al^{3+}, Si^{4+}, and Ca^{2+} from iron tailings could be promoted by both acid and alkali activation, and increased with the increase of acid concentration, whereas a higher alkali concentration would inhibit the ion dissolution. The crystallinity of biotite and quartz in iron tailings decreased to 9.82% and 24.4% after acid activation, and the high amorphous degree of these minerals indicating that the potential activity of iron tailings powder was greatly increased.

4. In summary, the iron tailings are suitable as fine aggregate and mineral admixture for cement mortar/concrete from the perspective of workability and strength. However, the durability of concrete prepared with iron tailings, especially with the acid-activated tailings powder, should be the future investigated. Moreover, the application of mechanical—chemical coupling-activated tailings in cement-based materials should be further compared and discussed.

Abbreviations

SEM–EDS	Scanning electron microscope with energy dispersive spectroscopy
XRD	X-ray diffraction
FTIR	Fourier transform infrared spectroscopy
TGA	Thermogravimetric analysis
EIS	Electrochemical impedance spectroscopy
FN, PS, CD, BD, LY	Iron tailings sand from different places of origin
TR	Natural river sand
ITZ	Interfacial transition zone
H1/3/5	Acid solution prepared with different solid dosages (1%, 3%, 5%)
N1/3/5	Alkali solution prepared with different solid dosages (1%, 3%, 5%)
G/D-FN/PS/CD/BD/LY/TR	Mortar prepared with different w/b ratios (0.48, 0.34) and sand
W–H/N-A/B/C-0/1/3/5	Iron tailings powder by different methods of activation
J	Control sample without iron tailings powder
W	Sample with unactivated iron tailings powder
NA3	Sample with alkali-activated tailings powder (method A and 3% dosage)
HB5	Sample with acid-activated tailings powder (method B and 5% dosage)
HB5NA3	Sample with acid–alkali coupling-activated tailings powder
CH	Calcium hydroxide
CSH	Hydrated calcium silicates

Author contributions
LK: conceptualization, supervision, writing—review and editing, project administration, and funding acquisition; SX: investigation, data curation, and writing—original draft; CW: methodology and formal analysis; LW: formal analysis. All authors read and approved the final manuscript.

Authors' information
Lijuan Kong is a professor, School of Materials Science and Engineering, Shijiazhuang Tiedao University, Shijiazhuang 050043, China. Shuheng Xie is a postgraduate, School of Materials Science and Engineering, Shijiazhuang Tiedao University, Shijiazhuang 050043, China. Caihui Wang is an associate professor, School of Materials Science and Engineering, Shijiazhuang Tiedao University, Shijiazhuang 050043, China. Lihuan Wang is an engineer, Hebei Institute of Civil Air Defence Works Design and Research, Shijiazhuang 050200, China.

Availability of data and materials
All data generated or analyzed during this study are included in this published article.

Declarations

Competing interests
There is no competing interest associated with the submission of this manuscript.

References
Adiguzel, D., Tuylu, S., & Eker, H. (2022). Utilization of tailings in concrete products: A review. *Construction and Building Materials., 360*, 129574.

Ashish, D. K. (2019). Concrete made with waste marble powder and supplementary cementitious material for sustainable development. *Journal of Cleaner Production, 211*, 716–729.

Ashish, D. K., & Verma, S. K. (2019). Cementing efficiency of flash and rotary-calcined metakaolin in concrete. *Journal of Materials in Civil Engineering, 31*(12), 04019307.

Cai, J., Zhang, S., & Hou, G. (2009). Effects of ferrous mill tailings as aggregates on workability and strength of concrete. *Journal of Wuhan University of Technology, 31*, 104–107.

Chen, B., Pang, L., Zhou, Z., et al. (2022). Study on the activation mechanism and hydration properties of gold tailings activated by mechanical—chemical—thermal coupling. *Journal of Building Engineering, 48*, 104014.

Cheng, Y., Huang, F., Li, W., et al. (2016). Test research on the effects of mechanochemically activated iron tailings on the compressive strength of concrete. *Construction and Building Materials, 118*, 164–170.

Kong *et al. Int J Concr Struct Mater* (2023) 17:24

Page 16 of 16

Duan, P., Shui, Z., Chen, W., et al. (2013). Effects of metakaolin, silica fume and slag on pore structure, interfacial transition zone and compressive strength of concrete. *Construction and Building Materials, 44*, 1–6.

Ishwarya, G., Singh, B., Deshwal, S., et al. (2019). Effect of sodium carbonate/sodium silicate activator on the rheology, geopolymerization and strength of fly ash/slag geopolymer pastes. *Cement and Concrete Composites, 97*, 226–238.

Jiang, F. (2008). *A study on the composition, structure and performance of slag-fines cementing materials alkali-activated, Xian*. Xian University of Architecture and Technology.

Kong, L., Hou, L., & Du, Y. (2014). Chemical reactivity of lightweight aggregate in cement paste. *Construction and Building Materials, 64*, 22–27.

Li, Y. (2003). *Study on composition, structure and properties of cement and concrete with steel-making slag powder mineral additive*. China Building Materials Academy.

Liu, X., Ni, C., Meng, K., et al. (2020). Strengthening mechanism of lightweight cellular concrete filled with fly ash. *Construction and Building Materials, 251*, 118954.

Losey, D. J., Sihvonen, S. K., Veghte, D. P., et al. (2018). Acidic processing of fly ash: Chemical characterization, morphology, and immersion freezing. *Environmental Science: Processes & Impacts, 20*(11), 1581–1592.

Ma, P., Li, X., Wen, Z., et al. (2021). Research progress on activation and mechanism of fly ash. *Inorganic Chemicals Industry, 53*(10), 28–35.

Mehta, A., & Ashish, D. K. (2020). Silica fume and waste glass in cement concrete production: A review. *Journal of Building Engineering, 29*, 100888.

Ping, X., Ping, G., Yan, F., et al. (1994). A.C. Impedance phenomena in hydrating cement systems: detectability of the high frequency arc. *Cement and Concrete Research, 24*(1), 92–94.

Pu, C. (2017). *Study on the activation process and mechanism of iron tailings powder and its influence on the performance of concrete*. Xuzhou: China University of Mining and Technology.

Saedi, A., Jamshidi-Zanjani, A., & Darban, A. K. (2020). A review on different methods of activating tailings to improve their cementitious property as cemented paste and reusability. *Journal of Environmental Management, 270*, 110881.

Saedi, A., Jamshidi-Zanjani, A., Mohseni, M., et al. (2023). Mechanical activation of lead–zinc mine tailings as a substitution for cement in concrete construction. *Construction and Building Materials, 364*, 129973.

Shettima, A. U., Hussin, M. W., Ahmad, Y., et al. (2016). Evaluation of iron ore tailings as replacement for fine aggregate in concrete. *Construction and Building Materials, 120*, 72–79.

Shi, C., Meyer, C., & Behnood, A. (2008). Utilization of copper slag in cement and concrete. *Resources, Conservation and Recycling, 52*, 1115–1120.

Song, G. (2000). Equivalence circuit model for AC electrochemical impedance spectroscopy of concrete. *Cement and Concrete Research, 30*(11), 1723–1730.

Thomas, B. S., Yang, J., Bahurudeen, A., et al. (2021). Sugarcane bagasse ash as supplementary cementitious material in concrete–A review. *Materials Today Sustainability, 15*, 100086.

Tian, J. (2010). *Study on proportion and applications of concrete with iron mine tailings*. Beijing: Tsinghua University.

USGS, United States Geological Survey— Mineral Commodity Summaries, Iron Ore, 2020.

Wu, R. (2020). *Performance and mechanism analysis of quartz type iron tailing powder and waste rock in cement-based materials*. Beijing: University of Science and Technology Beijing.

Yang, G., Deng, Y., & Wang, J. (2014). Non-hydrothermal synthesis and characterization of MCM-41 mesoporous materials from iron ore tailing. *Ceramics International, 40*, 7401–7406.

Yao, G., Wang, Q., Su, Y., et al. (2020). Mechanical activation as an innovative approach for the preparation of pozzolan from iron ore tailings. *Minerals Engineering, 145*, 106068.

Zhang, Y., Liu, B., Gu, X., et al. (2022). Mechanochemical activation of iron ore tailing-based ternary supplementary cementitious materials. *Construction and Building Materials, 346*, 128420.

Zhang, Z., Zhang, Z., Yin, S., et al. (2020). Utilization of iron tailings sand as an environmentally friendly alternative to natural river sand in high-strength concrete: Shrinkage characterization and mitigation strategies. *Materials, 13*(24), 5614.

Zhao, S., Fan, J., & Sun, W. (2014). Utilization of iron ore tailings as fine aggregate in ultra-high performance concrete. *Construction and Building Materials, 50*, 540–548.

Zhou, L., Gou, M., Hou, W., et al. (2022). Effect of thermal activation and particle size on cementitious activity of bauxite tailings. *Environmental Science and Pollution Research, 29*(52), 78960–78972.

Zhu, Q., Yuan, Y., Chen, J., et al. (2022). Research on the high-temperature resistance of recycled aggregate concrete with iron tailing sand. *Construction and Building Materials, 327*, 126889.

Publisher's Note

Springer Nature remains neutral with regard to jurisdictional claims in published maps and institutional affiliations.